

Dasatinib-induced spleen contraction leads to transient lymphocytosis

Ana Marcos-Jiménez,^{1,2} Daniela Claudino Carvoeiro,¹ Nora Ruef,¹ Carlos Cuesta-Mateos,² Emilia Roy-Vallejo,³ Valle Gómez-García de Soria,⁴ Claudio Laganá,⁵ Lourdes del Campo,^{5,6} Pablo Zubiaur,^{7,8} Gonzalo Villalpalos-García,⁷ Francisco Abad-Santos,^{7,8} Jens V. Stein,¹ and Cecilia Muñoz-Calleja^{2,6}

¹Department of Oncology, Microbiology and Immunology, University of Fribourg, Fribourg, Switzerland; ²Department of Immunology, Biomedical Research Institute La Princesa Hospital (IIS-IP), Madrid, Spain; ³Department of Internal Medicine, IIS-IP, Madrid, Spain; ⁴Department of Hematology, IIS-IP, Madrid, Spain; ⁵Department of Radiology, IIS-IP, Madrid, Spain; ⁶Department of Medicine, School of Medicine, Universidad Autónoma of Madrid, Madrid, Spain; ⁷Department of Clinical Pharmacology, University Hospital La Princesa, Teófilo Hernando Institute, Universidad Autónoma de Madrid, IIS-IP, Madrid, Spain; and ⁸Center for Biomedical Research Network on Liver and Digestive Diseases (CIBERehd), Health Research Institute Carlos III, Madrid, Spain

Key Points

- By promoting stromal cell contractility, dasatinib leads to a transient egress of lymphocytes from the spleen.
- Dasatinib-induced spleen resizing and lymphocyte mobilization open new possibilities for clinical applications.

The tyrosine kinase inhibitor dasatinib is approved for Philadelphia chromosome–positive leukemia, including chronic myeloid leukemia (CML). Although effective and well tolerated, patients typically exhibit a transient lymphocytosis after dasatinib uptake. To date, the underlying physiological process linking dasatinib to lymphocytosis remains unknown. Here, we used a small rodent model to examine the mechanism of dasatinib-induced lymphocytosis, focusing on lymphocyte trafficking into and out of secondary lymphoid organs. Our data indicate that lymphocyte homing to lymph nodes and spleen remained unaffected by dasatinib treatment. In contrast, dasatinib promoted lymphocyte egress from spleen with kinetics consistent with the observed lymphocytosis. Unexpectedly, dasatinib-induced lymphocyte egress occurred independently of canonical sphingosine-1-phosphate–mediated egress signals; instead, dasatinib treatment led to a decrease in spleen size, concomitant with increased splenic stromal cell contractility, as measured by myosin light chain phosphorylation. Accordingly, dasatinib-induced lymphocytosis was partially reversed by pharmacological inhibition of the contraction-promoting factor Rho- ρ associated kinase. Finally, we uncovered a decrease in spleen size in patients with CML who showed lymphocytosis immediately after dasatinib treatment, and this reduction was proportional to the magnitude of lymphocytosis and dasatinib plasma levels. In summary, our work provides evidence that dasatinib-induced lymphocytosis is a consequence of drug-induced contractility of splenic stromal cells.

Introduction

Chronic myeloid leukemia (CML) is characterized by the t(9;22) translocation, which results in the generation of the Philadelphia chromosome (Ph⁺) that encodes the oncogenic fusion protein BCR-ABL1. Dasatinib (BMS-354825, Bristol Myers Squibb) is a dual BCR-ABL/SRC inhibitor approved as the first-line treatment for adults and children with Ph⁺ CML and for patients with Ph⁺

Submitted 2 November 2022; accepted 16 December 2022; prepublished online on *Blood Advances* First Edition 30 December 2022; final version published online 26 May 2023. <https://doi.org/10.1182/bloodadvances.2022009279>.

Data are available on request from the corresponding authors, Jens V. Stein (jens.stein@unifr.ch) and Cecilia Muñoz-Calleja (cmunozc@salud.madrid.org).

The full-text version of this article contains a data supplement.

© 2023 by The American Society of Hematology. Licensed under [Creative Commons Attribution-NonCommercial-NoDerivatives 4.0 International \(CC BY-NC-ND 4.0\)](https://creativecommons.org/licenses/by-nc-nd/4.0/), permitting only noncommercial, nonderivative use with attribution. All other rights reserved.

acute lymphoblastic leukemia (ALL) in combination with chemotherapy.¹⁻⁴ Dasatinib is also being used as maintenance therapy after hematopoietic stem cell transplantation for patients with high-risk Ph⁺ ALL.⁵ Moreover, the future immunotherapeutic strategy of Ph⁺ ALL foresees the use of dasatinib in combination with monoclonal antibodies such as blinatumomab.^{6,7} Among many off-targets beyond the BCR-ABL core network, dasatinib inhibits the activities of the platelet-derived growth factor receptor (PDGFR), EphA2, c-KIT, and kinases involved in cytoskeleton and chromatin remodeling and in lymphocyte activation.⁸ Because of its broad spectrum, the therapeutic potential of dasatinib alone or in combination with other drugs is an exciting field of research. Proposed therapeutic uses of dasatinib include the treatment of solid tumors⁹⁻¹⁶ and T-cell lymphomas associated with the deregulation of T-cell receptor downstream pathways, that is, angioimmunoblastic T-cell lymphoma.¹⁵ Importantly, dasatinib seems to enhance the antitumor activity of chimeric antigen receptor (CAR) T cells by inhibiting their exhaustion driven by sustained tonic signaling.¹⁷ Recent publications proposed the use of dasatinib to control the activity and secondary effects associated with bispecific antibodies and CAR T cells,¹⁸⁻²⁰ in particular the life-threatening cytokine release syndrome. Indeed, a clinical trial is exploring the safety of combining CAR T-cell immunotherapy with dasatinib for B-cell malignancies (#NCT04603872).

Given its widening spectrum of applications in hematopoietic malignancies, it is of clinical relevance to fully characterize the impact of dasatinib treatment on the immune system of patients. In that respect, 1 of the most striking side effects of dasatinib in patients with CML or ALL (as well as healthy individuals) is an absolute leukocytosis, including a rapid rise in the number of circulating lymphocytes. This lymphocytosis peaks within the first 1 to 2 hours after oral drug intake and resolves spontaneously ~4 hours later, mirroring the short plasma half-life of dasatinib (4-6 hours).²¹ In a previous study, we confirmed that dasatinib-induced lymphocytosis was already present in most patients with CML after the first intake of dasatinib; lymphocytosis majorly comprised of an increased proportion of effector T cells and memory B cells, in addition to monocytes and other lymphocyte subsets, such as natural killer (NK) cells.²² Lymphocytosis positively correlates with the response to treatment,^{23,24} perhaps by promoting or restoring the function of leukemia-specific cytotoxic cells.²⁵ These observations raise the possibility of using dasatinib as a mobilizing and enhancer agent to treat other diseases, such as viral infections, including HIV-1 infection.²⁶ Yet, to date, the physiological process underlying dasatinib-induced lymphocytosis remains unclear.

The number of circulating lymphocytes is determined by the balance of (1) lymphocyte production in primary lymphoid organs; (2) their homing to secondary lymphoid organs (SLOs), such as spleen and lymph nodes (LNs), and, to a lesser extent, nonlymphoid organs; (3) their egress from these organs back to the blood; and (4) lymphocyte apoptosis. Given the rapid onset of lymphocytosis after dasatinib treatment, an effect on either lymphocyte homing and/or egress represents the most likely scenario. Homing into and egress out of SLOs are mediated by specialized chemokine and adhesion receptor molecules: CD62L, CCR7 (for T and B cells), CXCR4 and CXCR5 (for B cells), and LFA-1/VLA-4 integrins are key mediators of lymphocyte trafficking to LNs and spleen, whereas the sphingosine-1-phosphate receptor 1 (S1PR1) mediates lymphocyte egress from those organs. It is also conceivable that

dasatinib causes lymphocytosis in an indirect manner, for example, by affecting the stromal compartment of SLOs, which is composed of distinct subsets of CD45⁻ stromal cells including CD31⁺ podoplanin (PDPN)-negative blood endothelial cells (BECs), CD31⁻ PDPN⁺ fibroblastic reticular cells (FRCs), and CD31⁺ PDPN⁺ lymphatic endothelial cells (LECs; in LNs). In this context, a characteristic feature of FRCs and other lymphoid stromal cells is their ability to contract and expand, which enables them to rapidly adapt lymphoid organ size during infections.^{27,28} A central module of the cellular rheostat that regulates cellular contractility is the Rho-Rho-associated kinase (ROCK)-myosin light chain (MLC) axis. Upon activation of this cascade, MLC becomes phosphorylated to form pMLC, which results in increased contractility of the actomyosin cytoskeleton by activating nonmuscle myosin IIA.²⁹ Whereas these aforementioned publications have focused mostly on LNs, little is known about the behavior of stromal cells from the spleen during infections.

Here, we used a mouse model of dasatinib-induced lymphocytosis in combination with adoptive transfer of congenic reporter lymphocytes to examine the impact of drug treatment on homing into versus egress out of SLOs. Our data suggest that dasatinib does not affect the homing of lymphocytes to the spleen and LNs. In contrast, dasatinib treatment led to an S1PR1-independent lymphocyte egress from the spleen. This was accompanied by a decrease in spleen but not LN size and an increase in the splenic stromal cell contractility, as measured by elevated pMLC levels in various stromal cell subsets. Accordingly, dasatinib-induced lymphocytosis was partially reversed by inhibition of the contraction-promoting factor ROCK. Finally, we confirmed a reduction in spleen size after dasatinib treatment in patients with CML. In summary, our work provides insight into the mechanism underlying dasatinib-induced lymphocytosis, which further allows the mapping of the immunomodulatory effects caused by this drug.

Methods

Protocols for cell isolation and transfer and cell culture conditions as well as other general reagents used throughout the experiments are specified in supplemental Methods.

Mice

Male and female C57BL/6J mice, between 6 and 20 weeks old, from an in-house-bred colony or purchased from Janvier (AD Horst) were used in this study. CX3CR1 transgenic mice with green fluorescent protein (CX3CR1^{gfp+}) have been described previously.³⁰ All animals were maintained either at the University of Bern or the University of Fribourg (Switzerland). All animal work was approved by the Cantonal Committees for Animal Experimentation and conducted in accordance with federal guidelines.

Flow cytometry

Acquisition of the samples was performed using a BD FACSCanto II or a BD FACSLyric flow cytometry system, and data were analyzed using either FlowJo or Infinicyt software (version 2.0; Cytognos SL). The list of monoclonal antibodies and the gating strategies are specified in supplemental Methods.

Flow chamber assays

Murine T cells were pretreated with 100 nM dasatinib or dimethyl sulfoxide (DMSO) for 2 hours at 37°C and allowed to migrate in a

customized flow chamber (kind gift from Ruth Lyck) coated with rICAM-1/Fc (7.7 $\mu\text{g/mL}$, R&D Systems) and 2 μM CCL21 under shear flow conditions, as previously described.³¹ T-cell migration was recorded using an EC Plan Neofluar $\times 10/\text{NA}0.3$ objective coupled with a monochrome Charged Coupled Device (CCD) camera (AxioCam MRm Rev, Carl Zeiss). Time-lapse videos were recorded, 1 frame every 12 seconds (AxioVision, Carl Zeiss). Analysis was performed using Imaris software (Bitplane). The track speed is the average cellular velocity between the start and end of a track of a given cell.

Confocal microscopy

FRCs and spleens were imaged using a 4-laser (405 nm, 488 nm, 568 nm, and 647 nm) Leica SP5 spectral confocal scanning microscope fitted with a HyD detector (Leica Biosystems) and a PlanApo N 63 \times /1.40 NA oil microscope objective. Images were acquired with the LAS AF software (Leica) and analyzed using FIJI (National Institutes of Health). The detailed protocols are described in supplemental Methods.

Human samples

Fourteen patients with CML in current deep molecular response who were undergoing long-term treatment with dasatinib (median, 5.3 years) were recruited for this study, which was approved by the ethics committee of La Princesa University Hospital (register number 4294) in 2021. Informed consent was obtained from each participant. An echograph and a blood test were performed before and ~60 to 90 minutes after (median, 85 minutes) dasatinib intake. The examination was done using an Aplio ultrawideband convex transducer ultrasound (Canon; Tochigi, Japan). Preintake and postintake matching ultrasounds were performed by the same radiologist. Most patients were invited to participate a second time, to confirm results, and the first and second ultrasounds were performed by different radiologists, who remained blinded to the predicted outcome. The prolate ellipsoid formula was used to calculate the spleen volume (volume = length \times width \times thickness \times 0.52). A hemogram and immunophenotype test were performed with EDTA-anticoagulated blood samples. Plasma from these patients were frozen and used for later dasatinib level determinations with a fully validated high-performance liquid chromatography triple quadrupole mass spectrometry method.³²

Statistical analysis

Variables were described based on their mean and standard deviation. Normality was tested with a D'Agostino-Pearson test. Analyses were performed using GraphPad Prism software. For each experiment, the test is specified in the corresponding figure legend. $P < 0.05$ was considered statistically significant.

Results

Dasatinib induces lymphocytosis without affecting lymphocyte homing

To establish a model for dasatinib-induced leukocytosis, we treated C57BL/6 mice with dasatinib (50 mg/kg) and determined blood leukocyte counts 2 hours later using flow cytometry (Figure 1A). Dasatinib treatment caused an increase in total circulating leukocytes, particularly in CD4⁺/CD8⁺ T cells and B220⁺ B cells (Figure 1B). We also observed a nonsignificant trend in augmented

circulating neutrophils, monocytes, and NK cell numbers, in line with previous observations.⁹

In specific-pathogen-free (SPF) facility-housed C57BL/6 mice, most circulating lymphocytes display a naïve (CD62L⁺ CCR7⁺ CD44^{low}) phenotype and use the lymph and blood circulation systems to traffic between distinct SLOs.³³ We hypothesized that dasatinib-treated lymphocytosis might stem from either an impaired trafficking of blood-borne lymphocytes to SLOs, leading to their accumulation in blood, and/or an increased egress from SLOs. We therefore addressed the impact of dasatinib on lymphocyte homing. Ex vivo dasatinib treatment did not alter the expression of the chemokine receptors CCR7, CXCR4, and CXCR5, which bind lymphoid tissue-expressed chemokines, in B cells (supplemental Figure 1A) or T cells (data not shown). Furthermore, dasatinib exposure had no effect on the expression of the adhesion molecule CD62L required for initial attachment to high endothelial venules (HEVs) of LNs (supplemental Figure 1A) and did not induce lymphocyte apoptosis at the concentrations used (supplemental Figure 1B).

After CD62L-mediated rolling, lymphocytes crawl on CCL21- and ICAM-1-presenting HEVs under shear forces exerted by the blood flow before transmigrating into the LN parenchyme.³⁴ To address whether dasatinib can impair this process, we took advantage of a reductionist flow chamber model, in which naïve T cells migrate on an ICAM-1- and CCL21-coated surface under physiological shear flow conditions, resembling their interactions with HEVs. Quantification of their dynamic behavior failed to uncover significant differences between control and dasatinib-treated T lymphocytes during shear-induced detachment or on crawling frequency and speed, under these conditions (Figure 1C; supplemental Video 1).

To address the impact of dasatinib on in vivo lymphocyte homing, we treated fluorescently labeled T and B cells isolated from SLOs of C57BL/6 donor mice with DMSO or dasatinib for 2 hours before adoptive transfer. To control for a potential rapid reversal of dasatinib owing to its washing out after the transfer, we used control as well as 5 or 50 mg/kg dasatinib-treated C57BL/6 mice as recipients. Furthermore, we limited the homing window to 20 minutes after injection before isolating SLOs for flow cytometry analysis of transferred populations (Figure 1D). Similar ratios of DMSO and dasatinib-treated lymphocytes were recovered in peripheral and mesenteric LNs as well as in the spleen and blood of both types of recipients: those treated with the control and those with dasatinib (Figure 1E). Taken together, our data suggest that dasatinib causes lymphocytosis in a mouse model without impairing the homing capacity of lymphocytes.

Dasatinib promotes rapid lymphocyte egress from spleen

We examined whether dasatinib-induced lymphocytosis was linked to lymphocyte egress from SLOs. Given the natural variations in SLO cell numbers in individual mice, we adoptively transferred equal numbers of fluorescently labeled reporter-lymphocyte populations into untreated C57BL/6 recipient mice and allowed these cells to seed the SLO network of their hosts for 24 to 48 hours, when an equilibrium between homing and egress becomes established. On the day of the experiment (day 0), the recipients were treated with DMSO or dasatinib (50 mg/kg), or left untreated (for reference), and numbers of total and adoptively transferred CD4⁺, CD8⁺, and B220⁺ cells in SLOs were determined at 2 and

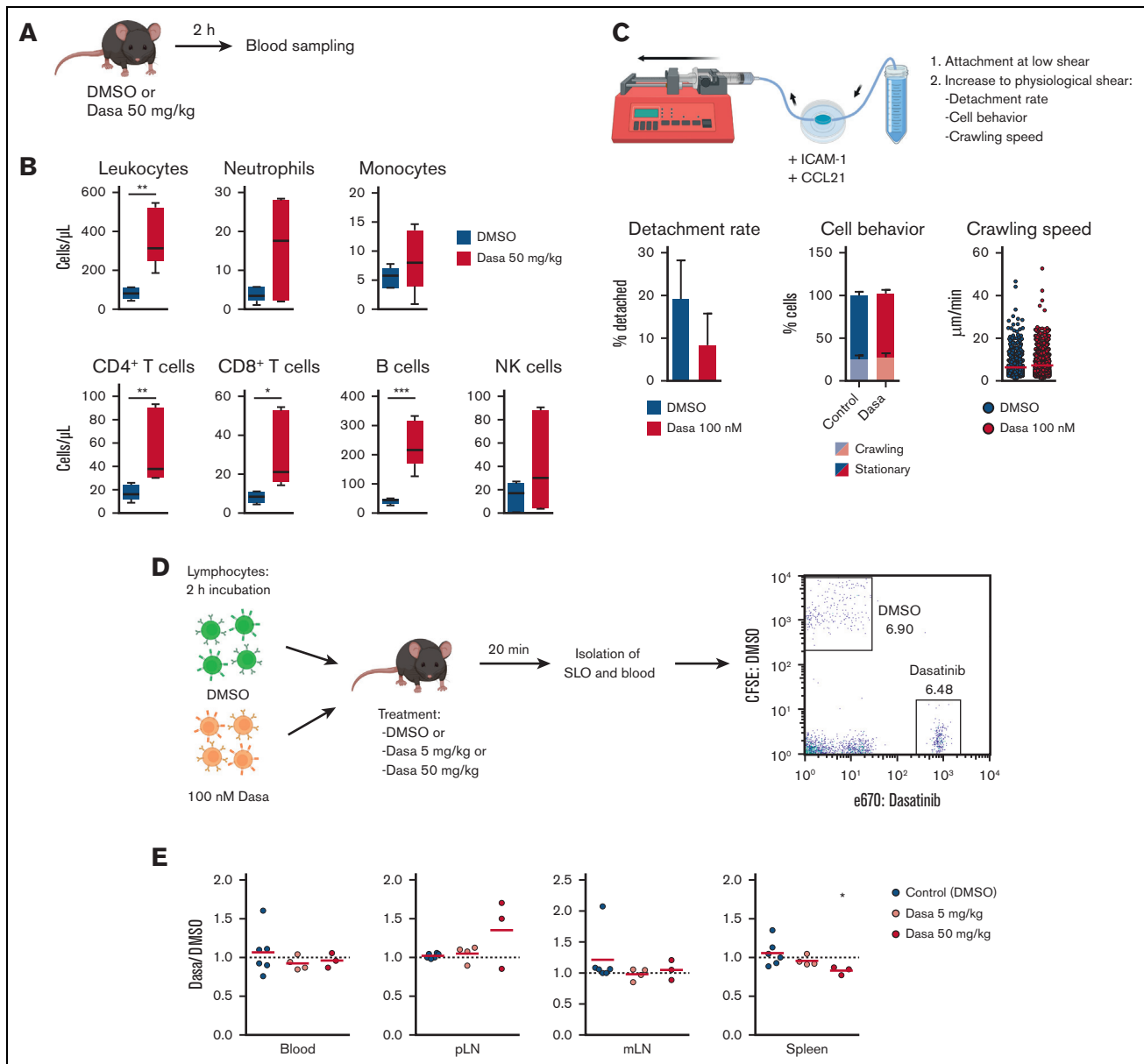


Figure 1. Dasatinib induces lymphocytosis without altering homing to SLOs. (A) Lymphocytosis assay in C57BL/6J mice. (B) Blood obtained 2 hours after the administration of DMSO (vehicle) or 50 mg/kg dasatinib (Dasa) was immunophenotyped to quantify leukocyte subpopulations by flow cytometry; $n = 5$ mice per group from 2 independent experiments. Boxplots depict 25th and 75th percentiles and the median, and the whiskers show fifth and 95th percentiles. Analyzed by Kruskal-Wallis test and Dunn multiple comparisons test. (C) Effect of dasatinib on adhesion and crawling of murine lymphocytes under shear flow. Detachment rate (percentage of detached cells after 5 minutes of high shear; mean \pm standard deviation) (left). Proportion of crawling and stationary cells (middle). Speed of crawling cells (right). $n = 3$; analyzed by Mann-Whitney U test. (D) Experimental layout for in vivo homing assay. (E) Ratio of dasatinib-treated and control (DMSO-treated) lymphocytes recovered for each organ. Red lines indicate the mean. A ratio of 1 indicates equal recovery. $n = 3$ independent experiments; analyzed by 1-sample t test. * $P < .05$; ** $P < .01$; *** $P < .001$. CFSE, carboxyfluorescein diacetate succinimidyl ester; mLN, mesenteric LN; pLN, peripheral LN.

6 hours after treatment (Figure 2A). In addition, we administered anti-CD62L monoclonal antibodies to determine egress from LNs. Our data uncovered that, as compared with recipients treated with DMSO, dasatinib treatment induced a significant reduction of reporter B-cell numbers in spleen as early as 2 hours after treatment (Figure 2B-C). Similarly, a decrease in reporter CD4⁺ and CD8⁺ T-cell numbers was observed (Figure 2B-C). A comparable but slightly delayed trend for dasatinib-induced cell number

decrease was observed for endogenous B- and T-cell populations (Figure 2B-C). A parallel examination of dasatinib-treated peripheral LNs, which included brachial and inguinal LNs, revealed a decline in reporter CD4⁺, CD8⁺, and B220⁺ cell counts as compared with DMSO-treated LNs, although this was less pronounced for endogenous cells (not shown). Taken together, these data suggest that dasatinib promotes the egress of lymphocytes from spleen and, to a lesser extent, from LNs.

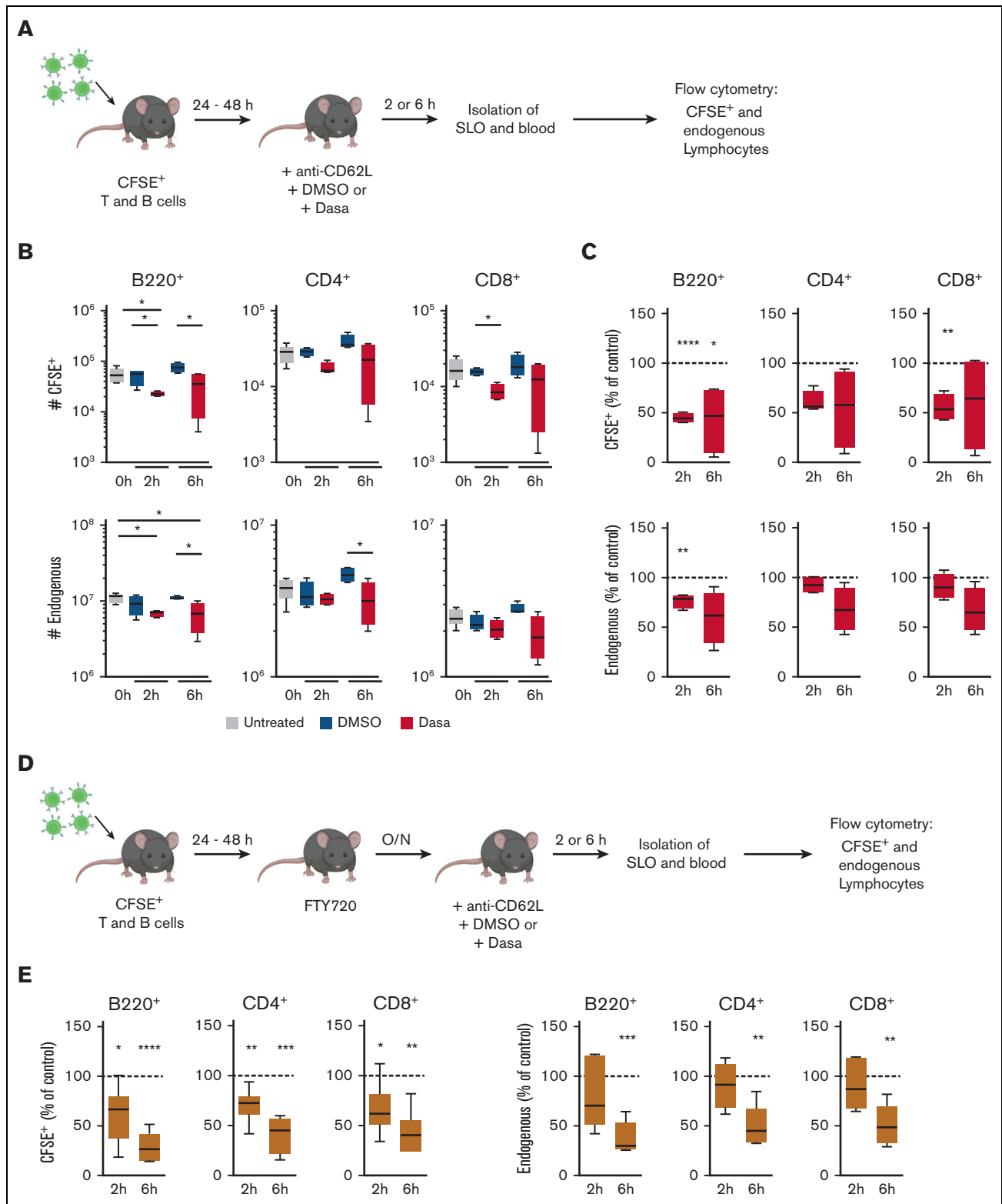


Figure 2. Dasatinib promotes lymphocyte egress from the spleen in a S1PR1-independent manner. (A) Experimental layout for egress assay. (B) Number of CFSE⁺ or endogenous B and T cells recovered from spleens of mice untreated or treated for 2 or 6 hours with DMSO or 50 mg/kg dasatinib. (C) Percentage of CFSE⁺ or endogenous cells recovered from spleens of dasatinib-treated mice normalized to DMSO-treated recipients (dotted line). $n = 4$ to 6 mice per group from 2 independent experiments; analyzed by 1-sample t test. (D) Experimental layout for egress assay in the presence of the S1PR1 agonist FTY720 (2 mg/kg). (E) Percentage of CFSE⁺ or endogenous cells normalized to DMSO-treated mice (dotted line). $n = 6$ mice per group from 3 independent experiments; analyzed by 1-sample t test. * $P < .05$; ** $P < .01$; *** $P < .001$. Boxplots depict 25th and 75th percentiles and the median, and the whiskers show fifth and 95th percentiles. O/N, overnight.

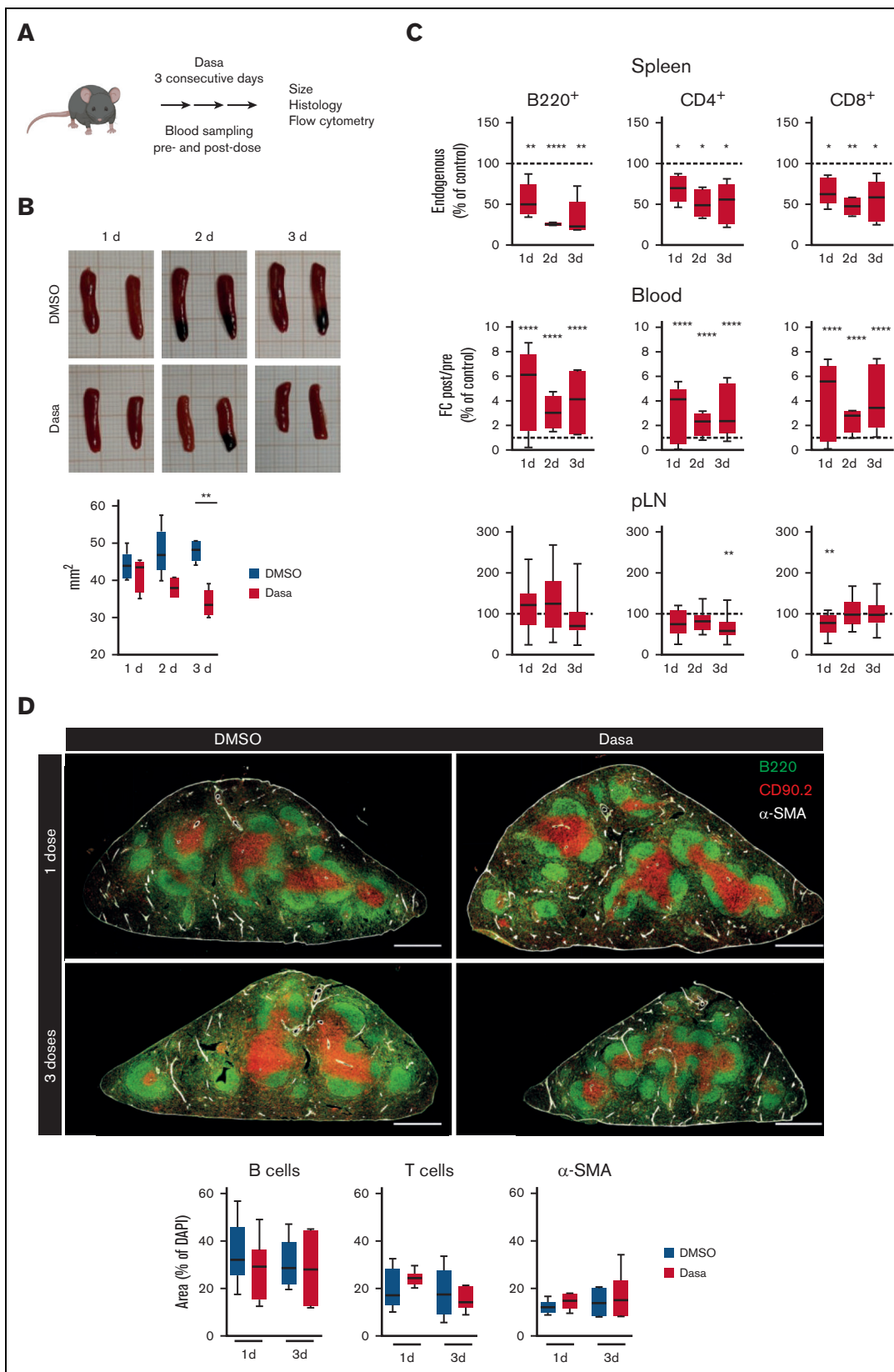


Figure 3. Dasatinib causes redistribution of lymphocytes and spleen shrinkage. (A) Experimental layout for the 3-day consecutive treatment with dasatinib. (B) Images from 1 representative experiment and spleen areas quantified using FIJI. Analyzed by Kruskal-Wallis test. (C) Endogenous B- and T-cell numbers are expressed as percentage of cells recovered from DMSO-treated mice. For blood, the fold change (FC) between posttreatment and pretreatment samples in dasatinib-treated mice was

To examine whether dasatinib treatment could also trigger the release of T cells from nonlymphoid tissues, we assessed whether dasatinib administration altered the frequency of CX3CR1⁺ CD8⁺ T cells, which participate in the surveillance of nonlymphoid tissue.³⁵ To generate CX3CR1⁺ CD8⁺ T cells in sufficient numbers for a quantitative analysis, we adoptively transferred CX3CR1^{gfp+}-expressing OT-I T cells into C57BL/6 recipients, which were subsequently challenged with lymphocytic choriomeningitis virus–ovalbumin, a replication-competent, attenuated lymphocytic choriomeningitis virus strain.³⁶ At >30 days after infection, we treated recipients with DMSO or dasatinib (50 mg/kg) and quantified the number of circulating CX3CR1^{gfp+} CD8⁺ T cells 2 hours later via flow cytometry analyses of blood samples. Dasatinib treatment did not increase the number of CX3CR1^{gfp+} CD8⁺ T cells as compared with control-treated recipients (supplemental Figure 2). This observation suggests that a substantial proportion of the dasatinib-induced increase in circulating lymphocytes is indeed derived from spleen and potentially other SLOs, rather than nonlymphoid organs.

Dasatinib-induced lymphocyte egress from spleen occurs independently of S1P1 signaling

We analyzed the mechanism underlying lymphocyte egress in more detail, focusing on the spleen as a major reservoir for lymphocytes. Because physiological lymphocyte egress from the spleen to the blood requires S1P,³⁷ and given the many off-target effects of dasatinib, we examined whether increased S1P responsiveness might precipitate T- and B-cell egress from the spleen. To address this point, we administered the functional S1PR1 antagonist FTY720 to mice that had received a fluorescently labeled lymphocyte reporter population. On the next day, we treated recipient mice with dasatinib or DMSO as control and examined reporter cell numbers as described earlier (Figure 2D). Although FTY720 treatment led to lymphopenia, confirming its efficacy (supplemental Figure 3), we again observed a decrease in endogenous and reporter cell numbers in spleen after dasatinib treatment (Figure 2E). These findings suggest that the mechanism of dasatinib-induced lymphocytosis occurs independently of the S1P-S1PR1 signaling axis.

Dasatinib causes a reduction in the spleen size

Given that the spleen is a dynamic organ, which can rapidly adapt its size during inflammation or physical exercise,³⁸ we determined whether dasatinib treatment affected organ size for mechanically driven lymphocyte egress. To mimic the daily uptake of medication in patients, we assessed the impact of dasatinib on the spleen and LN size after consecutive treatments. We treated C57BL/6 mice for 1, 2, or 3 days with dasatinib or DMSO and examined SLO size 2 hours after drug administration on a given day (Figure 3A) before processing them either for flow cytometry analysis of CD4⁺, CD8⁺, and B-cell numbers or for confocal microscopy. Already starting with the first dose of dasatinib, spleens showed a trend toward

smaller sizes, and this trend became statistically significant after the third dose (Figure 3B). Flow cytometry analysis helped confirm a decrease in the number of endogenous cells accompanied by a transient lymphocytosis after each individual treatment (Figure 3C). In contrast, LN sizes were not altered by dasatinib treatment (not shown), consistent with only mild changes in the number of endogenous lymphocytes in LNs (Figure 3C). Similarly, kidney sizes, as reference organ sizes, were unaffected by dasatinib treatment (not shown). Despite the decrease in size, the overall microenvironmental organization with clearly distinguishable B- and T-cell zones remained intact in dasatinib-treated spleens (Figure 3D). Taken together, these results suggest that dasatinib causes a decrease in spleen size, which correlates with a redistribution of lymphocytes to the circulation.

Dasatinib increases spleen stromal cell pMLC levels in a ROCK-dependent manner

Dasatinib treatment leads to an increase in actomyosin contractility in human endothelial cells,³⁹ and SLO stromal cells can rapidly regulate their contractility via a ROCK-pMLC pathway.²⁷ Given the rapid onset of spleen size reduction, we hypothesized that dasatinib might alter the contractility of splenic stromal cells. To determine whether the rapid decrease in spleen size correlates with altered actomyosin contractility, we used flow cytometry to assess stromal pMLC levels in the spleen and LNs at 2 hours after DMSO or dasatinib treatment (Figure 4A). In the CD45⁺ live singlet stromal cell populations, we examined BECs, LECs, FRCs, CD31⁺ PDPN⁺ CD157⁺ MAdCAM⁺ marginal reticular cells (MRCs), T-cell zone reticular cells (TRCs) defined as CD31⁺ PDPN⁺ CD157⁺ MAdCAM⁺ in LNs or CD31⁺ PDPN⁺ VCAM-1⁺ in the spleen, and CD31⁺ PDPN⁺ CD157⁺ MAdCAM⁺ medullary reticular cells (MedRCs in LNs) (supplemental Figure 4). Furthermore, we examined CD31⁺ PDPN⁺ VCAM-1⁺ and VCAM-1⁺ spleen stromal cell subsets, which may include both white and red pulp fibroblasts. In all spleen stromal cell subsets, we observed a tendency toward increased pMLC levels after dasatinib treatment, which reached statistical significance for BECs and TRCs. In contrast, LN stromal cells did not show increased pMLC levels after dasatinib treatment as compared with after DMSO (control) treatment (Figure 4B-C). Interestingly, LN MRC and TRC populations showed higher baseline pMLC levels than their splenic counterparts (Figure 4D).

Y27632 inhibits ROCK activity and has been experimentally used to lower cell contractility in cultured FRCs.²⁷ To examine whether Y27632 also reduced dasatinib-induced increases in pMLC levels, we used a murine FRC line and quantified their pMLC content via confocal microscopy, after the addition of dasatinib and/or Y27632. As predicted, Y27632 treatment resulted in cell spreading, accompanied by strongly reduced pMLC signal. In the presence of dasatinib, pMLC levels remained low in Y27632-treated FRCs as compared with control-treated FRCs,

Figure 3 (continued) normalized to that of the control mice (dotted line). $n = 4$ to 5 mice per group from 2 independent experiments; analyzed by 1-sample t test. (D) Representative confocal images from spleens of DMSO- or dasatinib-treated mice stained for B cells, T cells, or alpha-smooth muscle actin⁺ (α -SMA⁺) cells. The proportional area with respect to the total surface of the section was quantified with FUJI (4',6-diamidino-2-phenylindole [DAPI] staining represents 100%). Data pooled from at least 2 sections per mouse and a minimum of 3 mice per group. Scale bars represent 500 μ m. Analyzed using analysis of variance followed by Tukey multiple comparison test. * $P < .05$; ** $P < .01$; * $P < .05$; *** $P < .001$; **** $P < .0001$. Boxplots depict 25th and 75th percentiles and the median, and the whiskers show fifth and 95th percentiles.

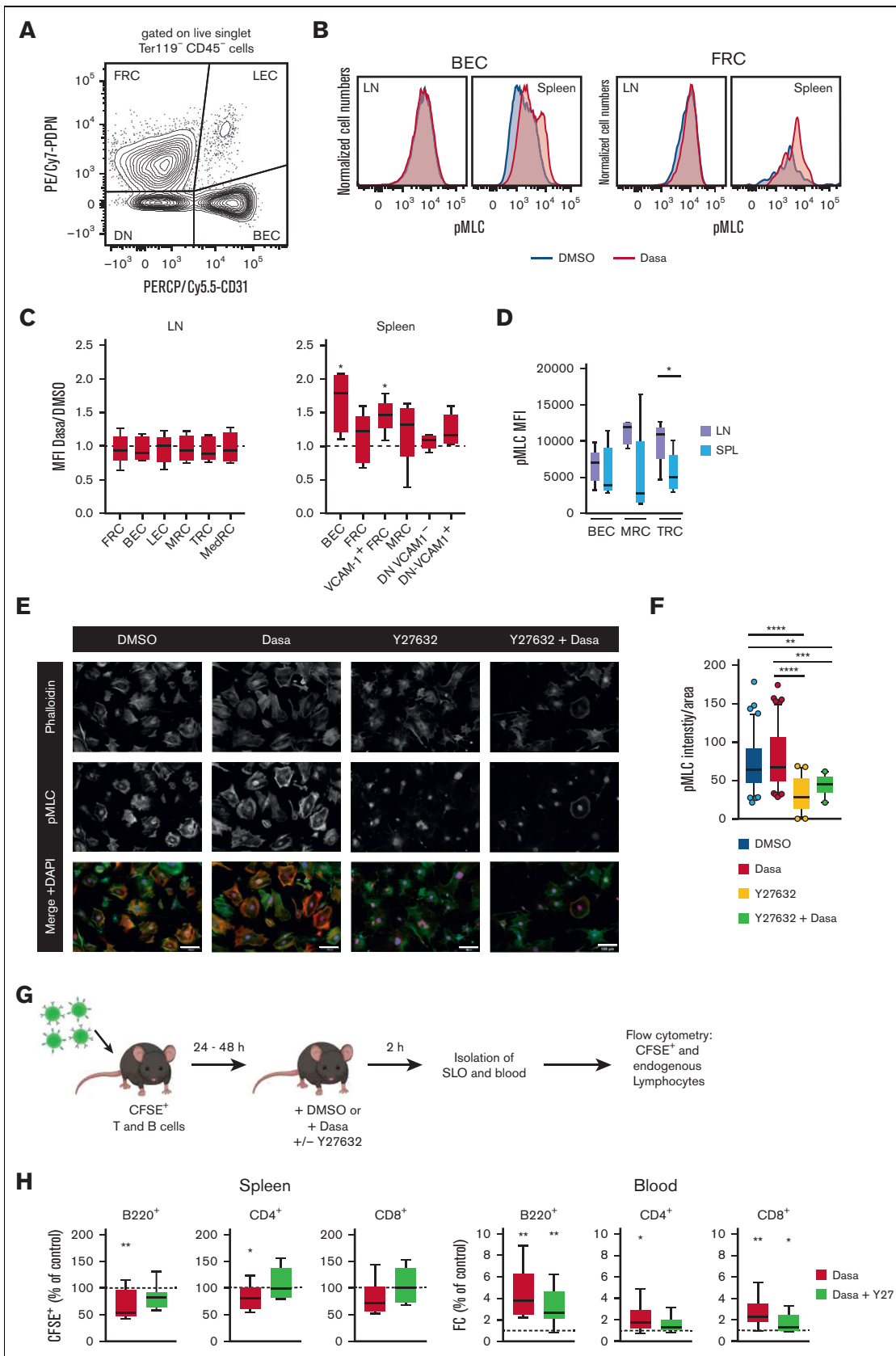


Figure 4.

suggesting that dasatinib acts upstream of ROCK to induce contraction (Figure 4E-F).

These data allowed us to examine whether Y27632 reversed the dasatinib-induced egress of a reporter population from spleen in vivo (Figure 4G). Indeed, coadministration of Y27632 reduced lymphocyte egress from the spleen, resulting in a similar recovery of reporter B and T cells from the spleen as that in recipients treated with DMSO (Figure 4H). Similarly, Y27632 treatment partially reverted dasatinib-induced lymphocytosis (Figure 4H). In summary, our data support a model in which dasatinib treatment leads to spleen contraction and release of lymphocytes into the blood, which is partially reversed by blocking ROCK activity.

Dasatinib induces rapid reduction of spleen sizes in patients with CML

To investigate whether the data obtained in our preclinical rodent model were reproducible in a clinical setting, we recruited a homogenous cohort of patients with CML ($n = 14$) in deep molecular response on chronic treatment with dasatinib (median, 5.3 years) in order to measure their spleens by ultrasound, before and after medication. The absence of splenomegaly at the time of analysis minimized the possibility of incorrectly attributing the decrease in spleen size within 1 hour after drug intake to a reduction in tumor burden. Total white blood cell and lymphocytes counts (including B cells, CD4 and CD8 T cells, and NK cells) were significantly increased in posttreatment samples, and the increase correlated with dasatinib concentration in plasma (Figure 5A; supplemental Figure 5A). In contrast, no changes in hematocrit, hemoglobin (Hb), or erythrocytes were observed (supplemental Figure 5B). A parallel ultrasound analysis of spleen uncovered a significant decrease of the 3 axis' (caudal, transverse, and anteroposterior) lengths after dasatinib treatment in most patients, which translated into a highly significant decrease in the total volume (Figure 5B). Importantly, the fold change in lymphocyte counts before and after dasatinib intake correlated with the percentage of the spleen volume reduction observed (Figure 5C; supplemental Figure 5C). Furthermore, we found a significant correlation between the plasma concentration of dasatinib and the level of the caudal axis (CA) reduction, which is the most robust readout by ultrasound (Figure 5C). Nonetheless, dasatinib dosage did not correlate with the percentage of volume or CA reduction, probably reflecting interpatient variability due to dose-to-weight ratio, because clinicians do not adjust the dose based on this parameter (supplemental Figure 5D). The percentage of volume change was negatively correlated with the duration of dasatinib treatment (Figure 5C), suggesting the development of some degree of tolerance to this effect after years of daily intake. In contrast,

long-term treatment was not associated with smaller spleen volumes or CA lengths (supplemental Figure 5E). In summary, our proof-of-concept study lends support to the hypothesis that dasatinib-triggered spleen contraction causes transient lymphocytosis.

Discussion

Tyrosine kinase inhibitors (TKIs) are widely used in the clinics to treat hematologic cancers, including CML, ALL, chronic lymphocytic leukemia, and some B-cell lymphomas. Based on vast clinical experience, links between TKIs' side effects (in addition to the effects on their specific targets) and patient prognosis are becoming increasingly appreciated. Because the degree of lymphocytosis caused by dasatinib has been associated with a better response in patients with CML, it is critical to understand the interference of dasatinib with the normal physiology of the human immune system and how this contributes to the cure of different malignancies. Here, we have determined the impact of dasatinib on noncancer cells in a preclinical small rodent model and patients with CML in deep molecular response. Our data suggest that dasatinib-induced lymphocytosis is mainly exerted via an indirect effect on stromal cell contractility in the spleen.

The number of circulating lymphocytes are determined by the homing and egress of lymphocytes into and out of SLOs. Our initial hypothesis was that dasatinib directly affects the homing capacity of lymphocytes because TKIs are able to impair lymphocyte homing to LNs.⁴⁰ In this context, lymphocytosis has been described for other TKIs, such as ibrutinib and idelalisib. The generally accepted mechanism for ibrutinib-induced B-cell lymphocytosis is a direct inhibition of adhesion and chemotaxis of malignant B cells to their survival niches, leading to their egress to the blood.^{41,42} For idelalisib, a decreased expression of CD62L on the leukemic cells, which contributes to a reduced homing capacity of these cells, has also been proposed.⁴³ Here, we did not find evidence for impaired recruitment of blood-borne lymphocytes to SLOs in the presence of dasatinib. Similarly, the microenvironmental organization of T- and B-cell compartments of dasatinib-treated organs remained preserved.

In contrast, our data show that dasatinib enhanced the egress from the spleen. Lymphocyte egress from LNs and the spleen is a tightly regulated process in which the balance between CCR7 and S1PR1 signaling plays a major role.⁴⁴⁻⁴⁶ Given that the treatment with the egress inhibitor FTY720 did not reverse the effect of dasatinib, the effect of dasatinib on lymphocyte egress most likely reflects a mechanical contraction of the organ. SLOs are highly plastic and have evolved to rapidly adapt their size to accommodate increasing numbers of leukocytes during inflammation, and to return to

Figure 4. Dasatinib increases spleen stromal cell pMLC levels in a ROCK-dependent manner. (A) Flow cytometry gating strategy for the main stromal cells analyzed after 2-hour treatment with dasatinib (50 mg/kg) or DMSO. (B) Representative example of pMLC expression in BECs and FRCs. (C) Ratio of pMLC expression of stromal cell subpopulations from LNs and spleens of dasatinib- and control-treated mice. Analyzed by 1-sample *t* test. (D) Mean fluorescence intensity (MFI) of pMLC from BECs, marginal reticular cells (MRCs), and TRCs recovered from LNs and spleens of DMSO-treated mice. $n = 5$ mice per group from 4 independent experiments. (E) Representative confocal images of subconfluent FRCs cultured on 20 $\mu\text{g}/\text{mL}$ of fibronectin and treated for 2 hours with DMSO, 100 nM dasatinib, 20 μM Y27632, or both inhibitors. Scale bars represent 100 μm . (F) Intensity of pMLC staining quantified by FIJI and normalized to the cell area. Each dot represents a cell. $n = 3$; analyzed by Kruskal-Wallis test. $*P < .05$; $**P < .01$; $***P < .001$; $****P < .0001$. (G) Experimental layout for egress assay in combination with Y27632. (H) Percentage of CFSE⁺ B cells and CD4⁺/CD8⁺ T cells recovered from the spleens, normalized to DMSO-treated mice (dotted line) (left). FC of CFSE⁺ B cells and CD4⁺/CD8⁺ T cells in blood of mice treated with dasatinib (50 mg/kg) alone, or dasatinib and Y27632 (10 mg/kg), normalized to DMSO-treated mice (dotted line) (right). $n = 9$ mice per group, from 3 independent experiments; analyzed by 1-sample *t* test. $*P < .05$; $**P < .01$; $***P < .001$; $****P < .0001$. Boxplots depict 25th and 75th percentiles and the median, and the whiskers show fifth and 95th percentiles. DN, CD31 PDPN double negative stromal cells; SPL, spleen.

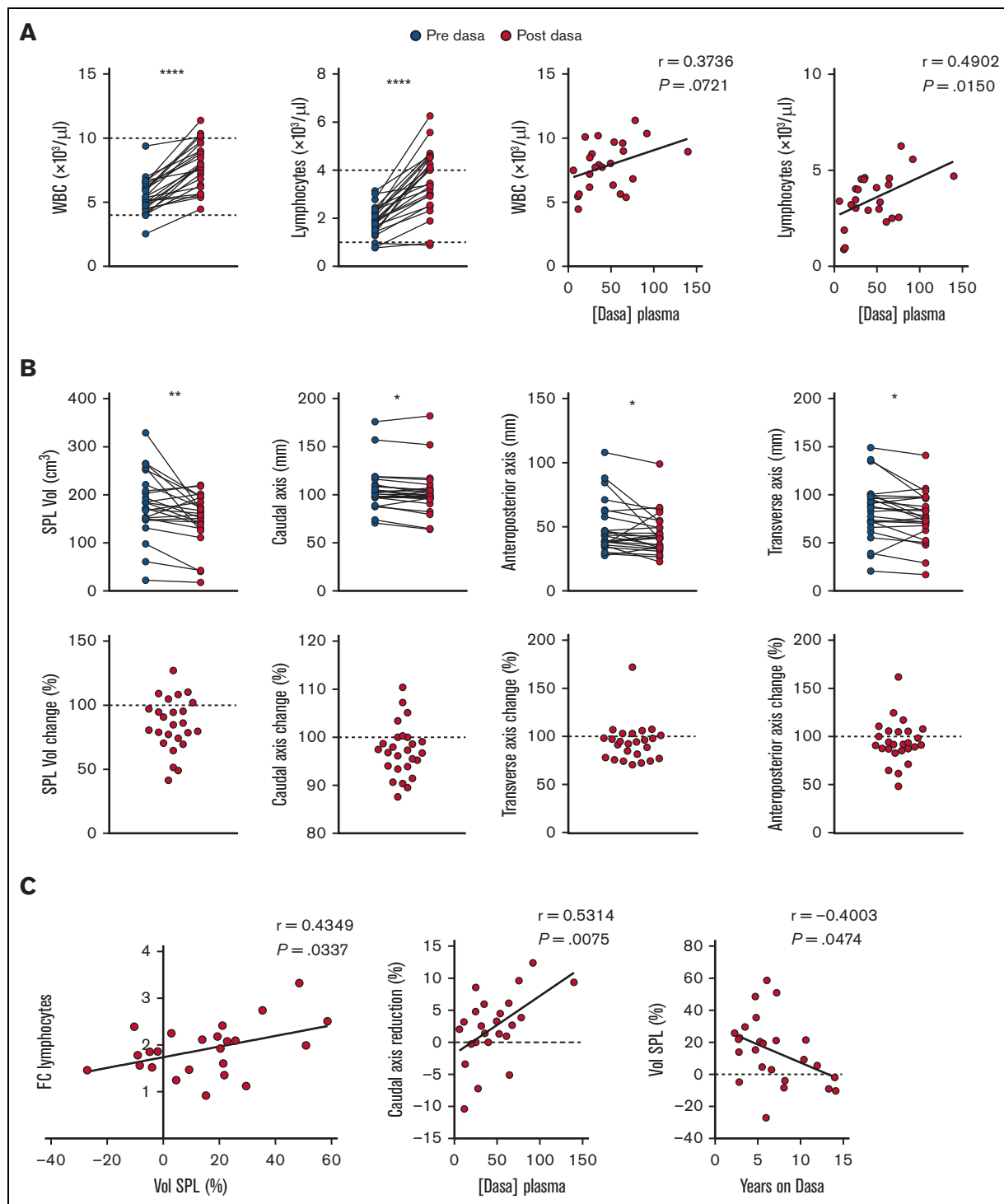


Figure 5. Dasatinib induces rapid reduction in spleen size in patients with CML. (A) A blood sample was withdrawn before and 1 hour after dasatinib intake and white blood cell (WBC) and lymphocyte numbers were quantified and correlated to dasatinib plasma concentration. (B) Quantification of the spleen volume (Vol), caudal (length), anteroposterior (width), and transverse (thickness) axes (upper row) before and after dasatinib intake. The lower row shows the percentage of change for each parameter. (C) Correlations between the FC of lymphocytes before and after dasatinib intake and the change of spleen volume shown as percentage of reduction, the change of CA shown as percentage of reduction and dasatinib plasma concentration, and between the change of spleen volume and years on dasatinib therapy. $n = 26$ determinations from 14 patients at different time points; analyzed by paired t test, Wilcoxon paired t test, and/or Pearson correlation coefficient, as appropriate. $*P < .05$; $**P < .01$; $*P < .05$; $***P < .001$; $****P < .0001$.

steady-state volume after clearance of infection. The mechanoproperties of tissues, which are influenced by contractility of the actomyosin cytoskeleton, are gaining increased attention in research. Previous work from our group showed that dasatinib causes ROCK activation in human umbilical endothelial cells, which in turn, increases the phosphorylation of MLC. This triggers activation of the nonmuscle myosin II, leading to actomyosin cytoskeleton contraction.³⁹ Although we only observed a minor increase in pMLC levels after dasatinib treatment in a cultured FRC line, we hypothesize that their adhesion to 2-dimensional tissue culture plates restricts substantial contraction. In turn, the 3-dimensional *in vivo* sponge-like stromal cell architecture of spleen might be more susceptible to contraction. Supporting this notion, α -SMA⁺ FRCs that populate lymphoid tissue are contractile cells.²⁷ In rodents and humans, splenic fibroblasts present in the red pulp as well as cells of the splenic capsule and trabeculae also express α -SMA.⁴⁷ A coordinated contraction of these cells represents a mechanism to explain transient lymphocytosis and spleen shrinkage. In line with this, systemic treatment with dasatinib caused enhanced levels of pMLC on different stromal cells populations from the spleen, including TRCs and BECs. In contrast, we did not observe a reduction in cell numbers or size of LNs. Several factors might play a role: firstly, the high baseline contractility of LN stromal cells may render these cells less susceptible to dasatinib-triggered contraction; and secondly, the LN volume is small compared with the larger spleen, and the collagen capsule may be comparably less flexible. Furthermore, the large number of lymphocytes that dasatinib mobilizes from the spleen into blood might trigger an increased influx into LNs, counteracting dasatinib-induced egress.

Spleen volume changes have previously been described in mammals as a mechanism through which to release erythrocytes for oxygen supply during physical activity such as diving and running.^{28,38} In this case, spleen contraction is mediated by G-protein-coupled adrenergic receptors, which, upon binding to their agonists, induce smooth muscle contraction. In humans, it is well described that the adrenaline response leads to spleen contraction, but whether it represents a reservoir of Hb has remained debatable.³⁸ Our data demonstrate that most patients show a reduction in spleen volume after dasatinib intake, concomitant with an increase in peripheral blood lymphocyte counts. Although no changes in Hb, hematocrit, or erythrocyte levels were found 1 hour after dasatinib intake, a catecholamine-induced spleen reduction cannot be excluded, because those parameters are reported to revert in shorter time spans.⁴⁸ Thus, an indirect effect of dasatinib on adrenergic regulation of lymphoid tissue irrigation and a direct effect on FRC contractility might have contributed to our observations. For example, a recent study reported an effect of catecholamine in LNs, inducing local hypoxia that translates into activation of calcium (Ca²⁺) signaling and ultimately leads to a decrease in lymphocyte motility.⁴⁹ In the future, it would be worth exploring whether dasatinib-induced changes in the concentration of cytoplasmic free Ca²⁺ could lead to Ca²⁺-calmodulin-triggered activation of the MLC kinase in FRCs. Another limitation of this study is that we did not examine in detail how dasatinib affects lymphocyte trafficking in skin- and gut-draining lymphoid tissue, and how dasatinib-induced spleen shrinkage affects local pro-survival niches of malignant cells. Likewise, we believe that it would be of interest to validate these findings in a larger cohort of newly diagnosed patients at baseline and during early follow-up to correlate the results with the outcome.

In summary, our data support a model underlying dasatinib-induced lymphocytosis via the induction of spleen shrinkage in a preclinical rodent model and in human participants. To our knowledge, this work provides novel insights that could be used in the future to better control the dasatinib-induced mobilization of both healthy and malignant lymphocytes. Given that daily mobilization of anti-tumor T cells may represent a common mechanism of dasatinib-induced immunosurveillance for different hematologic neoplasias, these observations are of clinical and translational relevance.

Acknowledgments

The authors acknowledge Ruth Lyck (Theodor Kocher Institute, University of Bern) for her help with the flow chamber assays; Hortensia de la Fuente and the Radiology Service staff of the University Hospital La Princesa for their collaboration with human data collection; Anna Kreutzman, Mette Illander, and Satu Mustjoki for their scientific discussion; and Sanjiv Luther (University of Lausanne) for providing FRC cell lines.

The graphical abstract was created with [BioRender.com](https://www.biorender.com).

This study was supported by research funding from the San Salvatore Foundation (J.V.S and C.M.-C.), the Swiss National Foundation (grants 31003A_172994 and 310030_200406) (J.V.S.), and the Institute of Health Carlos III (grant PI21/01803) (C.M.-C.), A.M.-J. was supported by research funding from Alfonso Martin Escudero Foundation and by the Institute of Health Carlos III (ISCIII) (grant CM19/00254) from the Spanish Ministry of Science Innovation and Universities and the European Regional Development Fund (ISCIII-FEDER) "A way to achieve Europe," which also supported E.R.-V. and G.V.-G. with the grants CM/00149 and FI20/00090, respectively. P.Z.'s contract with CIBERehd is financed by the Infraestructura de Medicina de Precisión asociada a la Ciencia y Tecnología (IMP/00009) (ISCIII).

Authorship

Contribution: A.M.-J. performed most experiments, analyzed the data, prepared the figures, and wrote the manuscript; D.C.C. analyzed stromal cell contractility *in vivo*; N.R. helped with *in vivo* experiments; C.C.-M. contributed to data analysis; E.R.-V. assisted in patient sample collection; V.G.-G.d.S. participated in patient recruitment; C.L. and L.d.C. performed the ultrasounds; P.Z., G.V.-G., and F.A.-S. measured dasatinib plasma levels; and J.V.S. and C.M.-C. designed and supervised the project, and wrote the manuscript with input from all coauthors.

Conflict-of-interest disclosure: The authors declare no competing financial interests.

ORCID profiles: A.M.-J., [0000-0002-7606-3580](https://orcid.org/0000-0002-7606-3580); D.C.C., [0000-0003-2348-3378](https://orcid.org/0000-0003-2348-3378); N.R., [0000-0001-5211-3363](https://orcid.org/0000-0001-5211-3363); E.R.-V., [0000-0001-5253-5785](https://orcid.org/0000-0001-5253-5785); L.d.C., [0000-0003-4787-7806](https://orcid.org/0000-0003-4787-7806); G.V.-G., [0000-0002-4849-3268](https://orcid.org/0000-0002-4849-3268); F.A.-S., [0000-0002-6519-8885](https://orcid.org/0000-0002-6519-8885); J.V.S., [0000-0002-8199-9586](https://orcid.org/0000-0002-8199-9586); C.M.-C., [0000-0003-4085-3115](https://orcid.org/0000-0003-4085-3115).

Correspondence: Cecilia Muñoz-Calleja, Biomedical Research Institute La Princesa Hospital (IIS-IP), Immunology Department, Calle Diego de León, 62. 28006, Madrid, Spain; email: cmunozc@salud.madrid.org; and Jens V. Stein, Faculty of Science and Medicine Section Oncology, Microbiology and Immunology (OMI) Chemin du Musée 5 CH - 1700 Fribourg; email: jens.stein@unifr.ch.

References

1. Kantarjian H, Shah NP, Hochhaus A, et al. Dasatinib versus imatinib in newly diagnosed chronic-phase chronic myeloid leukemia. *N Engl J Med*. 2010; 362(24):2260-2270.
2. Cortes JE, Saglio G, Kantarjian HM, et al. Final 5-year study results of DASISION: the dasatinib versus imatinib study in treatment-naïve chronic myeloid leukemia patients trial. *J Clin Oncol*. 2016;34(20):2333-1340.
3. U.S. Food and Drug Administration. Home page. Accessed 27 April 2021. <https://www.fda.gov/>
4. Ravandi F, O'Brien SM, Cortes JE, et al. Long-term follow-up of a phase 2 study of chemotherapy plus dasatinib for the initial treatment of patients with Philadelphia chromosome-positive acute lymphoblastic leukemia. *Cancer*. 2015;121(23):4158-4164.
5. Ravandi F, Othous M, O'Brien SM, et al. US intergroup study of chemotherapy plus dasatinib and allogeneic stem cell transplant in Philadelphia chromosome positive ALL. *Blood Adv*. 2016;1(3):250-259.
6. Saleh K, Fernandez A, Pasquier F. Treatment of Philadelphia chromosome-positive acute lymphoblastic leukemia in adults. *Cancers (Basel)*. 2022; 14(7):1805.
7. Foà R, Bassan R, Vitale A, et al. Dasatinib–blinatumomab for Ph-positive acute lymphoblastic leukemia in adults. *N Engl J Med*. 2020;383(17): 1613-1623.
8. Pan C, Olsen JV, Daub H, Mann M. Global effects of kinase inhibitors on signaling networks revealed by quantitative phosphoproteomics. *Mol Cell Proteomics*. 2009;8(12):2796-2808.
9. Hekim C, Ilander M, Yan J, et al. Dasatinib changes immune cell profiles concomitant with reduced tumor growth in several murine solid tumor models. *Cancer Immunol Res*. 2017;5(2):157-169.
10. Ceppi P, Papotti M, Monica V, et al. Effects of Src kinase inhibition induced by dasatinib in non-small cell lung cancer cell lines treated with cisplatin. *Mol Cancer Ther*. 2009;8(11):3066-3074.
11. Kopetz S, Lesslie DP, Dallas NA, et al. Synergistic activity of the Src family kinase inhibitor dasatinib and oxaliplatin in colon carcinoma cells is mediated by oxidative stress. *Cancer Res*. 2009;69(9):3842-3849.
12. Chen B, Xu X, Luo J, Wang H, Zhou S. Rapamycin enhances the anti-cancer effect of dasatinib by suppressing Src/PI3K/mTOR pathway in NSCLC cells. *PLoS One*. 2015;10(6):e0129663.
13. Walker S, Wankell M, Ho V, et al. Targeting mTOR and Src restricts hepatocellular carcinoma growth in a novel murine liver cancer model. *PLoS One*. 2019;14(2):e0212860.
14. ClinicalTrials.gov. ClinicalTrials.gov database search engine. Accessed 27 April 2021. <https://clinicaltrials.gov/>
15. Nguyen TB, Sakata-Yanagimoto M, Fujisawa M, et al. Dasatinib is an effective treatment for angioimmunoblastic T-cell lymphoma. *Cancer Res*. 2020; 80(9):1875-1884.
16. Umakanthan JM, Iqbal J, Batlevi CL, et al. Phase I/II study of dasatinib and exploratory genomic analysis in relapsed or refractory non-Hodgkin lymphoma. *Br J Haematol*. 2019;184(5):744-752.
17. Zhang H, Hu Y, Shao M, et al. Dasatinib enhances anti-leukemia efficacy of chimeric antigen receptor T cells by inhibiting cell differentiation and exhaustion. *J Hematol Oncol*. 2021;14(1):1-6.
18. Mestermann K, Giavridis T, Weber J, et al. The tyrosine kinase inhibitor dasatinib acts as a pharmacologic on/off switch for CAR T cells. *Sci Transl Med*. 2019;11(499):eaau5907.
19. Weber EW, Lynn RC, Sotillo E, Lattin J, Xu P, Mackall CL. Pharmacologic control of CAR-T cell function using dasatinib. *Blood Adv*. 2019;3(5): 711-717.
20. Leclercq G, Haegel H, Schneider A, et al. Src/lck inhibitor dasatinib reversibly switches off cytokine release and T cell cytotoxicity following stimulation with T cell bispecific antibodies. *J Immunother Cancer*. 2021;9(7):e002582.
21. Mustjoki S, Auvinen K, Kreutzman A, et al. Rapid mobilization of cytotoxic lymphocytes induced by dasatinib therapy. *Leukemia*. 2013;27(4):914-924.
22. Colom-Fernández B, Kreutzman A, Marcos-Jiménez A, et al. Immediate effects of dasatinib on the migration and redistribution of naïve and memory lymphocytes associated with lymphocytosis in chronic myeloid leukemia patients. *Front Pharmacol*. 2019;10:1340.
23. Schiffer CA, Cortes JE, Hochhaus A, et al. Lymphocytosis after treatment with dasatinib in chronic myeloid leukemia: effects on response and toxicity. *Cancer*. 2016;122(9):1398-1407.
24. Paydas S. Dasatinib, large granular lymphocytosis, and pleural effusion: useful or adverse effect? *Crit Rev Oncol Hematol*. 2014;89(2):242-247.
25. Kreutzman A, Juvonen V, Kairisto V, et al. Mono/oligoclonal T and NK cells are common in chronic myeloid leukemia patients at diagnosis and expand during dasatinib therapy. *Blood*. 2010;116(5):772-782.
26. Climent N, Plana M. Immunomodulatory activity of tyrosine kinase inhibitors to elicit cytotoxicity against cancer and viral infection. *Front Pharmacol*. 2019;10:1232.
27. Acton SE, Farrugia AJ, Astarita JL, et al. Dendritic cells control fibroblastic reticular network tension and lymph node expansion. *Nature*. 2014; 514(7253):498-502.
28. Vaahoteri K, Sixt M. Relax and come in. *Nature*. 2014;514(7523):441-442.

29. Vicente-Manzanares M, Ma X, Adelstein RS, Horwitz AR. Non-muscle myosin II takes centre stage in cell adhesion and migration. *Nat Rev Mol Cell Biol*. 2009;10(11):778-790.
30. Jung S, Aliberti J, Graemmel P, et al. Analysis of fractalkine receptor CX(3)CR1 function by targeted deletion and green fluorescent protein reporter gene insertion. *Mol Cell Biol*. 2000;20(11):4106-4114.
31. Coisne C, Lyck R, Engelhardt B. Live cell imaging techniques to study T cell trafficking across the blood-brain barrier in vitro and in vivo. *Fluids Barriers CNS*. 2013;10(1):7.
32. Koller D, Vaitsekhovich V, Mba C, et al. Effective quantification of 11 tyrosine kinase inhibitors and caffeine in human plasma by validated LC-MS/MS method with potent phospholipids clean-up procedure. Application to therapeutic drug monitoring. *Talanta*. 2020;208:120450.
33. Beura LK, Hamilton SE, Bi K, et al. Normalizing the environment recapitulates adult human immune traits in laboratory mice. *Nature*. 2016;532(7600):512-516.
34. Boscacci RT, Pfeiffer F, Gollmer K, et al. Comprehensive analysis of lymph node stroma-expressed Ig superfamily members reveals redundant and nonredundant roles for ICAM-1, ICAM-2, and VCAM-1 in lymphocyte homing. *Blood*. 2010;116(6):915-925.
35. Gerlach C, Moseman EA, Loughhead SM, et al. The chemokine receptor CX3CR1 defines three antigen-experienced CD8 T cell subsets with distinct roles in immune surveillance and homeostasis. *Immunity*. 2016;45(6):1270-1284.
36. Kallert SM, Darbre S, Bonilla W V, et al. Replicating viral vector platform exploits alarmin signals for potent CD8⁺ T cell-mediated tumour immunotherapy. *Nat Commun*. 2017;8:15327.
37. Ramos-Perez WD, Fang V, Escalante-Alcalde D, Cammer M, Schwab SR. A map of the distribution of sphingosine 1-phosphate in the spleen. *Nat Immunol*. 2015;16(12):1245-1252.
38. Stewart IB, McKenzie DC. The human spleen during physiological stress. *Sports Med*. 2002;32(6):361-369.
39. Kreutzman A, Colom-Fernandez B, Jimenez AM, et al. Dasatinib reversibly disrupts endothelial vascular integrity by increasing non-muscle myosin II contractility in a ROCK-dependent manner. *Clin Cancer Res*. 2017;23(21):6697-6707.
40. Stein JV, Soriano SF, M'Rini C, et al. CCR7-mediated physiological lymphocyte homing involves activation of a tyrosine kinase pathway. *Blood*. 2003;101(1):38-44.
41. De Rooij MFM, Kuil A, Geest CR, et al. The clinically active BTK inhibitor PCI-32765 targets B-cell receptor- and chemokine-controlled adhesion and migration in chronic lymphocytic leukemia. *Blood*. 2012;119(11):2590-2594.
42. Herman SEM, Mustafa RZ, Jones J, Wong DH, Farooqui M, Wiestner A. Treatment with ibrutinib inhibits BTK- and VLA-4-dependent adhesion of chronic lymphocytic leukemia cells in vivo. *Clin Cancer Res*. 2015;21(20):4642-4651.
43. Lafouresse F, Bellard E, Laurent C, et al. L-selectin controls trafficking of chronic lymphocytic leukemia cells in lymph node high endothelial venules in vivo. *Blood*. 2015;126(11):1336-1345.
44. Pham THM, Okada T, Matloubian M, Lo CG, Cyster JG. S1P1 receptor signaling overrides retention mediated by G alpha i-coupled receptors to promote T cell egress. *Immunity*. 2008;28(1):122-133.
45. Chauveau A, Pirogova G, Cheng HW, et al. Visualization of T cell migration in the spleen reveals a network of perivascular pathways that guide entry into T zones. *Immunity*. 2020;52(5):794-807.e7.
46. Matloubian M, Lo CG, Cinamon G, et al. Lymphocyte egress from thymus and peripheral lymphoid organs is dependent on S1P receptor 1. *Nature*. 2004;427(6972):355-360.
47. Steiniger BS. Human spleen microanatomy: why mice do not suffice. *Immunology*. 2015;145(3):334-346.
48. Schagatay E, Andersson JPA, Hallén M, Pålsson B. Selected contribution: role of spleen emptying in prolonging apneas in humans. *J Appl Physiol*. 2001;90(4):1623-1629.
49. Devi S, Alexandre YO, Loi JK, et al. Adrenergic regulation of the vasculature impairs leukocyte interstitial migration and suppresses immune responses. *Immunity*. 2021;54(6):1219-1230.e7.